

---

# ViG: Linear-complexity Visual Sequence Learning with Gated Linear Attention

---

Bencheng Liao<sup>1,2,◇</sup> Xinggang Wang<sup>2</sup>✉ Lianghai Zhu<sup>2</sup> Qian Zhang<sup>3</sup> Chang Huang<sup>3</sup>

<sup>1</sup> Institute of Artificial Intelligence, Huazhong University of Science & Technology

<sup>2</sup> School of EIC, Huazhong University of Science & Technology

<sup>3</sup> Horizon Robotics

<https://github.com/hustvl/ViG>

## Abstract

Recently, linear complexity sequence modeling networks have achieved modeling capabilities similar to Vision Transformers on a variety of computer vision tasks, while using fewer FLOPs and less memory. However, their advantage in terms of actual runtime speed is not significant. To address this issue, we introduce Gated Linear Attention (GLA) for vision, leveraging its superior hardware-awareness and efficiency. We propose direction-wise gating to capture 1D global context through bidirectional modeling and a 2D gating locality injection to adaptively inject 2D local details into 1D global context. Our hardware-aware implementation further merges forward and backward scanning into a single kernel, enhancing parallelism and reducing memory cost and latency. The proposed model, ViG, offers a favorable trade-off in accuracy, parameters, and FLOPs on ImageNet and downstream tasks, outperforming popular Transformer and CNN-based models. Notably, ViG-S matches DeiT-B’s accuracy while using only 27% of the parameters and 20% of the FLOPs, running 2× faster on 224 × 224 images. At 1024 × 1024 resolution, ViG-T uses 5.2× fewer FLOPs, saves 90% GPU memory, runs 4.8× faster, and achieves 20.7% higher top-1 accuracy than DeiT-T. These results position ViG as an efficient and scalable solution for visual representation learning.

## 1 Introduction

Vision Transformer (ViT) [18] has revolutionized computer vision by introducing an advanced sequence modeling layer Transformer [91] from natural language processing (NLP) to perform visual representation learning. It has proven highly successful across various vision tasks [58, 24, 23, 84, 75, 54, 50, 99, 22, 46, 69, 109, 25], serving as a versatile backbone. However, the quadratic complexity inherent in the Transformer’s softmax attention presents significant challenges for its applications on high-resolution images. Numerous efforts [58, 17, 105] have sought to address this limitation by drawing inspiration from the success of convolutional networks, such as constraining attention computations within local windows. While this approach achieves linear complexity similar to conventional CNNs, it falls short in capturing the global context. This raises a critical question: can we design a fundamental block that combines the best of both worlds—Transformers and CNNs—offering global receptive field and linear complexity?

The recent development of linear-time sequence modeling methods [28, 71, 106, 74, 85, 42] from NLP provides a promising solution to the question. These methods operate similarly to RNNs by compressing all historical inputs into a fixed-size state and then attending to the current input based on this compressed state, unlike Transformers [91] which attend to all historical states. To further

---

◇ Intern of Horizon Robotics when doing this work; ✉ Corresponding author: xgwang@hust.edu.cn

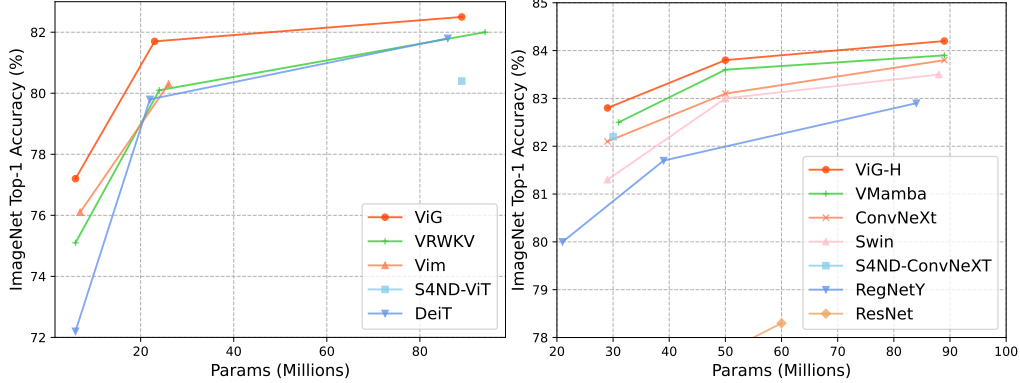
address the wall-time efficiency limitations of explicit recurrent forms, Mamba [28], RWKV [71], and GLA [106] introduce hardware-aware implementations, demonstrating superior accuracy and efficiency compared to highly-optimized Transformers. Mamba, in particular, has been widely adopted and adapted for vision tasks. While these methods achieve superior classification accuracy at a resolution of 224 and exhibit impressive efficiency in terms of FLOPs and memory at high resolutions (*e.g.*, 1248 resolution in Vision Mamba), their wall-time efficiency at lower and more common resolutions is often comparable to or even less than that of ViT/DeiT [18, 88].

This limitation inspires us to explore the application of the superior hardware-efficient GLA [106, 107] to push the efficiency and accuracy envelope of linear-complexity visual sequence learning, making it more practical and competitive with the well-established and highly-optimized Transformers and CNNs. Different from Mamba based on SISO (single-input-single-output) state space model [29], GLA originates from linear attention [42], which has a simple and hardware-friendly matrix-multiply form by approximating softmax in standard attention with a linear kernel. To further enhance the expressiveness, GLA introduces a novel data-dependent gating mechanism to adaptively control the forget rate of compressed state.

However, the vanilla GLA model is designed for unidirectional modeling, which has temporal dependence. This makes its ability for global perception in NLP not truly global when applied to vision tasks. Despite some follow-up works [38, 104, 40] on Mamba in vision that explore additional scanning directions beyond bidirectional modeling of 1D visual sequences to approximate vanilla attention’s ability to interact with visual tokens in any direction and position, these approaches suffer from significant memory inefficiencies due to frequent, non-sequential memory access patterns, making them less practical in terms of wall-time efficiency. We adhere to bidirectional modeling for its simplicity and memory-friendly access pattern. To further harness the inherent directional sensitivity in vision data (*i.e.*, information from different visual directions varies significantly in importance), we propose a bidirectional GLA (BiGLA) layer by designing a direction-wise gating mechanism to adaptively select the global context from different directions. This design shares most parameters between the forward and backward directions. Though the proposed directional design achieves global context along the 1D visual sequence, it still fails to capture the 2D nature of visual data. To address this, we propose a 2D gating locality injection to adaptively compress 2D local information extracted by convolution into the 1D global context extracted by the sequence modeling BiGLA layer. Moreover, the proposed parameter-efficient bidirectional design allows us to merge bidirectional scanning into a single kernel, enhancing the hardware-awareness of the implementation and reducing memory cost and latency introduced by the extra direction.

The main contributions of this paper can be summarized as follows:

- We present ViG, a generic vision backbone network that combines the linear complexity of Gated Linear Attention (GLA) with the hardware-awareness needed for efficient visual sequence learning. ViG addresses the limitations of previous Transformer-based and CNN-based methods, combining the best of both worlds to offer an efficient and scalable solution.
- To better adapt to vision tasks, we propose three key designs with minimal overhead: a bidirectional gated linear attention mechanism to capture the global 1D context of visual sequences, a direction-wise gating mechanism to adaptively select global context from different directions, and a 2D gating locality injection to integrate 2D local information into the 1D global context. We further provide a hardware-aware implementation that merges forward and backward scanning into a single kernel, enhancing parallelism and reducing memory cost and latency.
- Our models achieve superior performance in terms of accuracy and parameters compared to state-of-the-art non-hierarchical and hierarchical models on ImageNet [14], as shown in Fig. 1. For downstream dense prediction tasks [116, 52], ViG outperforms ViT [18, 88] and VRWKV [19] with lower computational costs across different model sizes. The wall-time efficiency of ViG outperforms the counter-part linear-complexity visual sequence learning methods [117, 19, 56] and matches the well-established and highly-optimized ConvNeXt [59] and SwinTransformer [58].



(a) Comparison with non-hierarchical architectures

(b) Comparison with hierarchical architectures

Figure 1: Performance comparisons of (a) non-hierarchical architectures [19, 88, 117, 66] and (b) hierarchical architectures [56, 59, 58, 66, 77, 32] on ImageNet-1K. Our proposed non-hierarchical ViG and hierarchical ViG-H demonstrate superior performance compared to the popular models in terms of parameters and accuracy. Particularly, the proposed basic ViG block achieves global receptive field with linear complexity, while the CNN [32, 77, 59], vanilla softmax attention [88] and window-attention-based [58] blocks cannot.

## 2 Related Work

ViT [18] demonstrated that visual representation learning can be performed in a sequence manner by introducing the Transformer [91] from NLP. Many follow-up works [97, 96, 105, 9, 20, 21, 30, 17, 90, 112, 57, 110, 8, 113, 48] focus on improving ViT’s efficiency and performance without altering the softmax attention. Recently, another line of works [35, 74, 42, 7, 1, 73, 10, 13, 65, 62] have shown that quadratic softmax attention can be replaced by advanced RNN-like, linear-time sequence modeling methods. Vision Mamba [117] builds upon the linear-time sequence modeling Mamba block [28] by introducing an additional backward SSM layer. VMamba [56] introduces criss-cross scanning to Mamba and builds a hierarchical architecture. LocalMamba [40] optimizes scanning directions to exploit local priors for vision. Zigma [38] and PlainMamba [104] introduce multiple scanning directions in a zigzag manner. Many works [60, 47, 4, 51, 102, 115, 114, 68, 82, 108, 33, 26, 5] have explored Mamba’s effectiveness in various vision tasks. In contrast, VisionRWKV [19] forgoes the Mamba block, adapting the linear complexity RWKV block from NLP for use in vision. Extended related works are provided in Appendix A.

## 3 Preliminary

In this section, we introduce the evolution from standard softmax attention to advanced gated linear attention (GLA), omitting the multi-head mechanism for simplicity.

**Softmax Attention.** Softmax attention has been used as a standard block in Transformer [91] since it has the strong capability to dynamically model the relationship across long sequence and enjoys great parallelism for training. Given an input sequence  $\mathbf{X} \in \mathbb{R}^{T \times d}$ , the softmax attention used in autoregressive Transformer can be defined as:

$$\begin{aligned} \mathbf{Q}, \mathbf{K}, \mathbf{V} &= \mathbf{X}\mathbf{W}_Q, \mathbf{X}\mathbf{W}_K, \mathbf{X}\mathbf{W}_V, \\ \mathbf{O} &= \text{softmax}((\mathbf{Q}\mathbf{K}^\top) \odot \mathbf{M})\mathbf{V}, \end{aligned} \quad (1)$$

where  $\mathbf{W}_Q \in \mathbb{R}^{d \times d_q}$ ,  $\mathbf{W}_K \in \mathbb{R}^{d \times d_k}$  and  $\mathbf{W}_V \in \mathbb{R}^{d \times d_v}$  are trainable projection matrices,  $\mathbf{M} \in \{-\infty, 1\}^{T \times T}$  is the causal mask for preventing interaction with future tokens,  $\mathbf{O} \in \mathbb{R}^{T \times d_v}$  is the output. The above parallel form can also be written in the following recurrent form to compute the single output  $\mathbf{o}_t$ :

$$\begin{aligned} \mathbf{q}_t, \mathbf{k}_t, \mathbf{v}_t &= \mathbf{x}_t\mathbf{W}_Q, \mathbf{x}_t\mathbf{W}_K, \mathbf{x}_t\mathbf{W}_V, \\ \mathbf{o}_t &= \frac{\sum_{i=1}^t \exp(\mathbf{q}_t\mathbf{k}_i^\top)\mathbf{v}_i}{\sum_{i=1}^t \exp(\mathbf{q}_t\mathbf{k}_i^\top)}, \end{aligned} \quad (2)$$

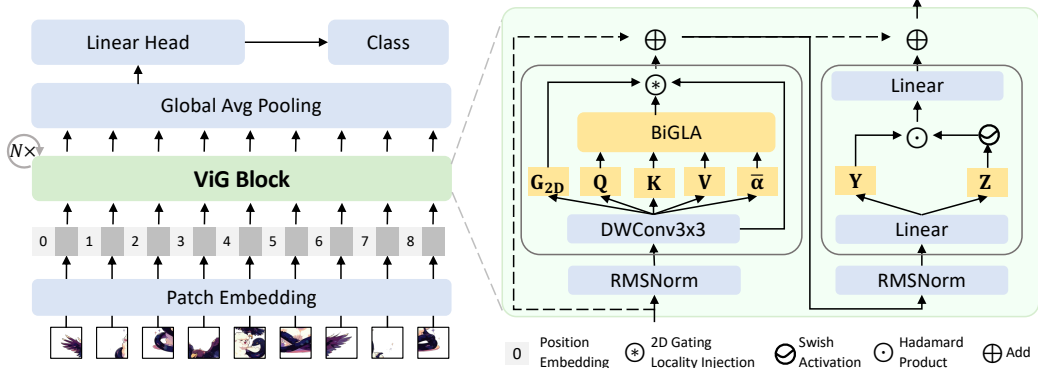


Figure 2: The overall architecture of ViG. We follow ViT [18] to build architecture by first transforming the input image into a sequence of patches and then feeding it into  $N$  basic ViG blocks. The proposed ViG block consists of RMSNorm [111], the proposed linear complexity spatial mixing layer, and SwiGLU Feed Forward Network [81].

where the output  $o_t$  is computed by attending the projected query  $q_t$  of  $x_t$  to the sets of projected keys  $\{k_1, \dots, k_t\}$  and values  $\{v_1, \dots, v_t\}$ .

**Linear Attention.** Linear attention [42] replaces  $\exp(q_t k_i^\top)$  in standard softmax attention with feature map dot-products  $\phi(q_t)\phi(k_i)^\top$ . Recently, [72] has empirically found that linear feature map works well by setting  $\phi$  to be the identity and removing the normalizer. This simplifies the computation of  $o_t$  as:

$$o_t = q_t \sum_{i=1}^t k_i^\top v_i. \quad (3)$$

Letting hidden state  $S_t = \sum_{i=1}^t k_i^\top v_i \in \mathbb{R}^{d_k \times d_v}$ , which is fixed-size and compresses the historical information, we can rewrite above computation as an RNN:

$$S_t = S_{t-1} + k_t^\top v_t, \quad o_t = q_t S_t. \quad (4)$$

**Gated Linear Attention.** [106] propose adding a data-dependent gating mechanism in linear attention to enhance expressiveness. The gated linear attention can be defined as:

$$\begin{aligned} \alpha_t &= \text{sigmoid}((x_t W_\alpha^1 W_\alpha^2 + b_\alpha))^{\frac{1}{\tau}} \in \mathbb{R}^{1 \times d_k}, \\ \mathbf{G}_t &= \alpha_t^\top \mathbf{1} \in (0, 1)^{d_k \times d_v}, \\ S_t &= \mathbf{G}_t \odot S_{t-1} + k_t^\top v_t \in \mathbb{R}^{d_k \times d_v}, \\ o_t &= q_t S_t, \end{aligned} \quad (5)$$

where  $\alpha_t$  is obtained from applying a low-rank linear layer on  $x_t$  followed by sigmoid activation,  $W_\alpha^1 \in \mathbb{R}^{d \times 16}$ ,  $W_\alpha^2 \in \mathbb{R}^{16 \times d_k}$ ,  $b_\alpha \in \mathbb{R}^{1 \times d_k}$  are trainable matrices and  $\tau = 16$  is a temperature term to encourage the model to have a slower forgetting rate,  $\mathbf{G}_t$  is matrix-form forget gate, expanded by outer-producting with matrix  $\mathbf{1}$ .

## 4 Method

### 4.1 Overall Architecture

The overall architecture of our model is depicted in Fig. 2. We first transform the  $H \times W \times 3$  image into  $T = \frac{H \times W}{p^2}$  patch tokens with  $d$  dimensions, where  $p$  is the patch size. Before feeding the patch tokens into the stack of ViG blocks, we add learnable position embeddings. The output tokens of the last block are fed into a global average pooling layer followed by a linear classifier.

### 4.2 ViG Block

ViG block, serving as a basic block, consists of: 1) a long-term BiGLA layer that can exploit the 1D-global context of the image in a linear-complexity manner; 2) a short-term depth-wise convolution

layer that can capture the 2D-local details of the image; 3) a gating mechanism that can adaptively combine the global and local information; 4) a SwiGLU FFN layer as in [89, 85, 106] for channel mixing.

#### 4.2.1 Global Bidirectional Gated Linear Attention

In this work, we adopt bidirectional modeling for its inherent simplicity and memory-friendly access pattern. The crux of this design is the direction-wise gating mechanism, particularly the forget gate  $\mathbf{G}_t$ , which meticulously controls the flow of information. This is crucial, especially for tokens located at the boundaries of an object, where information from different directions varies significantly in importance. To harness this directional sensitivity effectively, we introduce the Bidirectional Gated Linear Attention (BiGLA) layer, as shown in Fig. 3. This layer is parameter-efficient by sharing all parameters except for the forget gate, which is tailored to each direction:

$$\begin{aligned}
\bar{\alpha}_t &= \text{sigmoid}((\mathbf{x}_t \mathbf{W}_\alpha^1 \bar{\mathbf{W}}_\alpha^2 + \bar{\mathbf{b}}_\alpha))^{\frac{1}{2}} \in \mathbb{R}^{1 \times 2d_k}, \\
\vec{\alpha}_t, \overleftarrow{\alpha}_t &= \text{split}(\bar{\alpha}_t) \in \mathbb{R}^{1 \times d_k}, \\
\vec{\mathbf{G}}_t &= \vec{\alpha}_t^\top \mathbf{1} \in (0, 1)^{d_k \times d_v}, \\
\overleftarrow{\mathbf{G}}_t &= \overleftarrow{\alpha}_t^\top \mathbf{1} \in (0, 1)^{d_k \times d_v}, \\
\vec{\mathbf{S}}_t &= \vec{\mathbf{G}}_t \odot \vec{\mathbf{S}}_{t-1} + \mathbf{k}_t^\top \mathbf{v}_t \in \mathbb{R}^{d_k \times d_v}, \\
\overleftarrow{\mathbf{S}}_t &= \overleftarrow{\mathbf{G}}_t \odot \overleftarrow{\mathbf{S}}_{t+1} + \mathbf{k}_t^\top \mathbf{v}_t \in \mathbb{R}^{d_k \times d_v}, \\
\vec{o}_t &= \mathbf{q}_t \vec{\mathbf{S}}_t, \\
\overleftarrow{o}_t &= \mathbf{q}_t \overleftarrow{\mathbf{S}}_t, \\
o_t &= (\vec{o}_t + \overleftarrow{o}_t)/2,
\end{aligned}$$

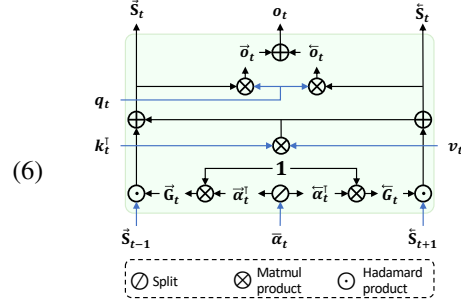


Figure 3: Illustration of BiGLA.

where  $\bar{\square}$  indicates bidirectional modification,  $\vec{\square}$  and  $\overleftarrow{\square}$  indicate forward and backward direction respectively,  $\bar{\mathbf{W}}_\alpha^2 \in \mathbb{R}^{16 \times 2d_k}$  and  $\bar{\mathbf{b}}_\alpha \in \mathbb{R}^{1 \times 2d_k}$ . The proposed BiGLA layer compresses the historical information of forward and backward directions into fixed-size hidden states  $\vec{\mathbf{S}}_t$  and  $\overleftarrow{\mathbf{S}}_t$ , and attends  $\mathbf{q}_t$  with the hidden states to obtain long-term global context in a linear-complexity manner.

The proposed design only introduces extra  $17d_k$  parameters to render vanilla causal GLA layer into BiGLA layer for visual representation learning, which is minor compared to the total  $4d^2$  parameters (roughly) by setting  $d_q, d_k = \frac{d}{2}$  and  $d_v = d$ . The designed BiGLA layer has nearly the same number of parameters as the standard softmax attention while using much fewer FLOPs ( $\Omega_{\text{BiGLA}} = 5Td^2 + 32Td$  vs.  $\Omega_{\text{SoftmaxAttn}} = 4Td^2 + 2T^2d$ ).

#### 4.2.2 2D Gating Locality Injection

Though the hidden states  $\vec{\mathbf{S}}_t$  and  $\overleftarrow{\mathbf{S}}_t$  in the BiGLA layer, compressed along the 1D visual sequences, can capture the long-term global context of the image, they may find it difficult in capturing the local details of 2D images. To address this issue, we inject 2D locality by introducing a short-term local convolution layer. In our case, we use  $3 \times 3$  depthwise convolution for its efficiency in parameters and FLOPs, where the  $3 \times 3$  convolutional filters are separated into each channel. Inspired by the data-dependent gating mechanism in GLA [106], we propose a data-dependent gating aggregation for 2D locality injection to interleave the global and local information:

$$\begin{aligned}
\mathbf{O}_{\text{local}} &= \text{DWConv}_{3 \times 3}(X), \\
\mathbf{O}_{\text{global}} &= \text{BiGLA}(\mathbf{O}_{\text{local}}), \\
\mathbf{G}_{2D} &= \text{sigmoid}(\mathbf{O}_{\text{local}} \mathbf{W}_{\text{gate2D}} + \mathbf{b}_{\text{gate2D}}), \\
\mathbf{O} &= \mathbf{G}_{2D} \odot \mathbf{O}_{\text{local}} + (\mathbf{1} - \mathbf{G}_{2D}) \odot \mathbf{O}_{\text{global}}.
\end{aligned} \tag{7}$$

### 4.3 Architecture Details

Equipped with the proposed ViG block, we mainly investigate two kinds of variants of ViG: ViT-style non-hierarchical models with a fixed number of tokens in each block and CNN-style hierarchical models with gradually downsampled tokens.

For ViT-style models, we set the patch size  $p$  to 16 and stack 12 ViG blocks. Then, we obtain 3 variants of the model at different sizes (ViG-T, ViG-S, and ViG-B) by directly adjusting the embedding dimension  $d$ , which have similar parameters to DeiT-T, S, and B. For hierarchical models, we also propose 3 variants (ViG-H-T, ViG-H-S, and ViG-H-B) following the design of SwinTransformer. We set the patch size  $p$  to 4 and apply our proposed ViG block at different stages. The detailed architectures are provided in Appendix B.

#### 4.4 Efficient Implementation

The practical efficiency of the model not only depends on the theoretical FLOPs but is mostly determined by the hardware-awareness of the implementation. It means the implemented model should: 1) be aware of memory hierarchy; 2) leverage the specialized compute unit (tensor cores on GPU for fast matrix multiplication); 3) have a high degree of parallelism. Thanks to the hardware-aware implementation of GLA, the most calculation-intensive parts of ViG can be represented in matrix multiplication and are performed on faster SRAM instead of slower high bandwidth memory (HBM), leading to superior wall-time efficiency by leveraging the tensor cores and reducing the HBM I/O cost.

**Hardware-aware Bidirectional Design.** Given the multi-directional nature of representing 2D images in 1D flattened sequences, the pioneering work Vim, based on bidirectional modeling, chooses to invoke two sequential kernels to process the forward and backward directions separately, which is inefficient in terms of parallelism. In this work, we propose a hardware-aware bidirectional design by fusing the forward and backward directions of Eq. (6) into a single kernel to achieve higher parallelism. Moreover, owing to the parameter-efficient design of the BiGLA layer, we can reduce the materialization of the backward visual sequence in high-bandwidth memory (HBM), which saves on memory costs.

## 5 Experiment

We conduct extensive experiments to validate the effectiveness of our proposed models. We present the main results on ImageNet [14] and compare them with various other models. Additionally, we benchmark our model on downstream dense prediction tasks, including object detection on the COCO [52] dataset and semantic segmentation on ADE20K [116].

### 5.1 Image Classification

**Settings.** We train classification experiments on ImageNet-1K dataset, which is a widely used large-scale benchmark for image classification. To fairly compare with previous works, we mainly follow the training and evaluation setting of DeiT and SwinTransformer [88, 58]. Specifically, all the models are trained from scratch for 300 epochs. Images are cropped to  $224 \times 224$  for both training and evaluation. Further details are provided in Appendix C.

**Comparison with Non-hierarchical Architectures.** Tab. 1 compares ViG with plain non-hierarchical architectures based on different sequence modeling layers, including Transformer, SSM, and linear RNN. The results show that the proposed ViG achieves superior trade-off in terms of parameters and accuracy across various model sizes, as shown in Fig. 1 (a). Remarkably, ViG-S has nearly the same number of parameters as DeiT-S and significantly outperforms it by 1.9% top-1 accuracy, which matches the performance of DeiT-B (only 0.1% lower) with  $3.7\times$  fewer parameters,  $5\times$  fewer FLOPs and  $2\times$  faster throughput. Moreover, ViG-B reaches 82.6% top-1 accuracy, surpassing DeiT-B by 0.8%, VRWKV-B by 0.6%, and S4ND-ViT-B by 2.2%.

In terms of practical throughput, ViG surpasses other linear-complexity sequence modeling methods, notably being  $1.8\times$  faster than Vim-T and  $1.6\times$  faster than Vim-S at tiny and small model sizes respectively. Compared with the counterparts with multi-direction scanning, ViG-T is  $5.2\times$  faster than LocalVim-T and  $4.6\times$  faster than PlainMamba-L1 thanks to the memory-friendly access pattern of bidirectional modeling. ViG is only slightly slower than DeiT, which can be attributed to the high parallelism of the Transformer and the low FLOPs when inputting small  $224 \times 224$  images. As shown in Fig. 4, ViG achieves exponential superiority as the image size increases.

**Comparison with Hierarchical Architectures.** Tab. 1 compares ViG-H with hierarchical architectures, including the advanced CNN-based RegNet and ConvNeXt, as well as Transformer-based Swin

Table 1: Comparison with plain non-hierarchical architectures (left) and hierarchical architectures (right) on ImageNet-1K validation set. “Size” means train/val image size. “#P.”, “Tp.”, and “Acc.” denote the number of parameters, throughput and top-1 accuracy respectively. Tp. (images/s) is measured on a single 4090 GPU with batch size 256 following [58].

Method	Size	#P.	FLOPs	Tp.	Acc.	Method	Size	#P.	FLOPs	Tp.	Acc.
<b>Transformers</b>						<b>Convnets</b>					
ViT-B/16 [18]	384 <sup>2</sup>	86M	55.4G	-	77.9	RegNetY-4G [77]	224 <sup>2</sup>	12M	4G	-	80.0
ViT-L/16 [18]	384 <sup>2</sup>	307M	190.7G	-	76.5	RegNetY-8G [77]	224 <sup>2</sup>	25M	8G	-	81.7
DeiT-T [88]	224 <sup>2</sup>	6M	1.3G	5761	72.2	RegNetY-16G [77]	224 <sup>2</sup>	45M	16G	-	82.9
DeiT-S [88]	224 <sup>2</sup>	22M	4.6G	2396	79.8	EffNet-B3 [86]	300 <sup>2</sup>	12M	1.8G	-	81.6
DeiT-B [88]	224 <sup>2</sup>	86M	17.6G	837	81.8	EffNet-B4 [86]	380 <sup>2</sup>	19M	4.2G	-	82.9
<b>MLP</b>						EffNet-B5 [86]	456 <sup>2</sup>	30M	9.9G	-	83.6
gMLP-T [53]	224 <sup>2</sup>	6M	1.4G	3872	72.3	EffNet-B6 [86]	528 <sup>2</sup>	43M	19.0G	-	84.0
gMLP-S [53]	224 <sup>2</sup>	20M	4.5G	1676	79.6	EffNet-B7 [86]	528 <sup>2</sup>	66M	37.0G	-	84.3
gMLP-B [53]	224 <sup>2</sup>	73M	15.8G	647	81.6	ConvNeXt-T [59]	224 <sup>2</sup>	29M	4.5G	1505	82.1
<b>SSMs</b>						ConvNeXt-S [59]	224 <sup>2</sup>	50M	8.7G	905	83.1
S4ND-ViT-B [66]	224 <sup>2</sup>	89M	-	562	80.4	ConvNeXt-B [59]	224 <sup>2</sup>	89M	15.4G	643	83.8
Vim-T [117]	224 <sup>2</sup>	7M	1.5G	2561	76.1	<b>Transformers</b>					
Vim-S [117]	224 <sup>2</sup>	26M	5.1G	1151	80.3	Swin-T [58]	224 <sup>2</sup>	28M	4.6G	1511	81.3
LocalVim-T [40]	224 <sup>2</sup>	8M	1.5G	885	76.2	Swin-S [58]	224 <sup>2</sup>	50M	8.7G	915	83.0
LocalVim-S [40]	224 <sup>2</sup>	28M	4.8G	396	81.2	Swin-B [58]	224 <sup>2</sup>	88M	15.4G	661	83.5
PlainMamba-L1 [104]	224 <sup>2</sup>	7M	3.0G	995	77.9	<b>SSMs</b>					
PlainMamba-L2 [104]	224 <sup>2</sup>	26M	8.1G	482	81.6	S4ND-ConvNeXt-T [66]	224 <sup>2</sup>	30M	-	643	82.2
PlainMamba-L3 [104]	224 <sup>2</sup>	51M	14.4G	279	82.3	VMamba-T [56]	224 <sup>2</sup>	31M	4.9G	1161	82.5
<b>Linear RNN</b>						VMamba-S [56]	224 <sup>2</sup>	50M	8.7G	779	83.6
VRWKV-T [19]	224 <sup>2</sup>	6M	1.2G	4551	75.1	VMamba-B [56]	224 <sup>2</sup>	89M	15.4G	577	83.9
VRWKV-S [19]	224 <sup>2</sup>	24M	4.6G	1724	80.1	EfficientVMamba-B [70]	224 <sup>2</sup>	33M	4.0G	1258	81.8
VRWKV-B [19]	224 <sup>2</sup>	94M	18.2G	635	82.0	LocalVMamba-T [40]	224 <sup>2</sup>	26M	5.7G	330	82.7
<b>Linear Attention</b>						LocalVMamba-S [40]	224 <sup>2</sup>	50M	11.4G	193	83.7
ViG-T	224 <sup>2</sup>	6M	0.9G	4645	77.2	<b>Linear Attention</b>					
ViG-S	224 <sup>2</sup>	23M	3.5G	1886	81.7	ViG-H-T	224 <sup>2</sup>	29M	4.5G	1480	82.8
ViG-B	224 <sup>2</sup>	89M	13.8G	701	82.6	ViG-H-S	224 <sup>2</sup>	50M	8.8G	890	83.8
						ViG-H-B	224 <sup>2</sup>	89M	15.5G	621	84.2

Transformer, and SSM-based S4ND and VMamba. Thanks to the linear complexity of the proposed VGLA block, ViG-H achieves similar FLOPs to those of window-based Transformers and CNNs, but with the added advantage of a global receptive field. As shown in Fig. 1 (b), ViG-H achieves the best top-1 accuracy across different model sizes.

The results of practical throughput demonstrate that ViG-H surpasses the SSM-based S4ND and VMamba, and matches the performance of well-established and highly-optimized ConvNeXt and SwinTransformer.

## 5.2 Object Detection

**Settings.** We conduct experiments for object detection and instance segmentation on the COCO 2017 dataset [52]. We utilize Mask-RCNN [31] as the detection head and follow VRWKV [19] to integrate the ViT-Adapter [6] on our plain ViG models. Further details are provided in Appendix C.

**Results.** In Tab. 2, for high-resolution  $1333 \times 800$  input images, ViT needs to resort to window attention to ensure efficiency, sacrificing accuracy. Unlike ViT, ViG can efficiently process high-resolution images directly with a global receptive field. The results demonstrate that ViG outperforms both ViT and VRWKV in terms of FLOPs and accuracy. Specifically, ViG-T uses only half the backbone FLOPs of ViT-T but achieves 1.7 higher AP<sup>b</sup> and 1.2 higher AP<sup>m</sup>, surpassing VRWKV-T by 1.6 in AP<sup>b</sup> and 1.1 in AP<sup>m</sup>. For the base model size, though VRWKV-B is more efficient than ViT-B in FLOPs, it still falls short of ViT-B by 0.1 in AP<sup>m</sup>. Meanwhile, our ViG-B achieves 0.5 higher AP<sup>b</sup> and 0.4 higher AP<sup>m</sup> than ViT-B with 44% lower backbone FLOPs.

Table 2: Object detection and instance segmentation on COCO val2017 (left) & semantic segmentation on ADE20K val set (right). “#Param” denotes the number of backbone parameters. “FLOPs” in the left and right tables denote the computational workload of the backbone with an input image of  $1333 \times 800$  and  $512 \times 512$ , respectively. “†” means window attention is adopted in ViT layers. “‡” denotes that the results of Vim are directly taken from its paper since it uses the same segmentation head and training recipe as ours.

Method	#Param.	FLOPs	AP <sup>b</sup>	AP <sup>m</sup>	Method	#Param.	FLOPs	mIoU
ViT-T <sup>†</sup>	8M	95.4G	41.1	37.5	Vim-T <sup>‡</sup>	-	-	41.0
ViT-T	8M	147.1G	41.6	37.9	ViT-T	8M	20.9G	42.6
VRWKV-T	8M	67.9G	41.7	38.0	VRWKV-T	8M	16.6G	43.3
ViG-T	8M	<b>61.2G</b>	<b>43.3</b>	<b>39.1</b>	ViG-T	8M	<b>14.9G</b>	<b>43.8</b>
ViT-S <sup>†</sup>	28M	241.2G	44.6	39.7	Vim-S <sup>‡</sup>	-	-	44.9
ViT-S	28M	344.5G	44.9	40.1	ViT-S	28M	54.0G	46.2
VRWKV-S	29M	189.9G	44.8	40.2	VRWKV-S	29M	46.3G	47.2
ViG-S	28M	<b>164.1G</b>	<b>45.5</b>	<b>40.8</b>	ViG-S	28M	<b>40.0G</b>	<b>47.9</b>
ViT-B <sup>†</sup>	100M	686.7G	46.2	41.5	ViT-B	100M	157.9G	48.8
ViT-B	100M	893.3G	46.8	41.8	VRWKV-B	107M	146.0G	49.2
VRWKV-B	107M	599.0G	46.8	41.7	ViG-B	103M	<b>121.5G</b>	<b>49.4</b>
ViG-B	103M	<b>498.5G</b>	<b>47.3</b>	<b>42.2</b>				

Table 3: **Roadmap of ViG.** The throughput and memory are measured on a single NVIDIA RTX 4090 GPU with batch size 256 and image size 224 following [58].

Method	Roadmap	#Param.	Throughput	Memory	Top-1 Acc.
DeiT	-	5.72M	5761	627MB	72.2
GLA	-	5.72M	6662	582MB	66.1
+	improved patch embedding layer	5.75M	6634	582MB	73.8
+	direct bidirectional modeling	5.75M	4564	748MB	75.2
+	absolute position embedding	5.79M	4571	748MB	75.4
+	direction-wise $\bar{\alpha}$ (§4.2.1)	5.81M	4566	785MB	76.3
+	2D gating locality injection (§4.2.2)	5.83M	3812	842MB	77.2
+	hardware-aware bidirection impl. (§4.4)	5.83M	4645	730MB	77.2

### 5.3 Semantic Segmentation

**Settings.** We train experiments for semantic segmentation on the ADE20K [116] dataset. We use UperNet [98] as the segmentation head and adopt the ViT-Adapter [6] following VRWKV [19] to adapt our plain ViG for segmentation. Training details are the same as VRWKV [19] and Vim [117], which are detailed in the Appendix C.

**Results.** As shown in Tab. 2, for medium-resolution  $512 \times 512$  input images, ViG outperforms the quadratic-complexity Transformer-based ViT and the linear-complexity RNN-based VRWKV across different model sizes in both FLOPs and segmentation accuracy. For instance, in the tiny size models, ViG outperforms ViT by 1.2 mIoU and 5G FLOPs, and VRWKV by 0.5 mIoU and 1.7G FLOPs. In the small size models, ViG surpasses ViT by 1.7 mIoU and 14G FLOPs, and VRWKV by 0.7 mIoU and 6.3G FLOPs. These results demonstrate ViG’s superior adaptability for dense-pixel prediction tasks compared to VRWKV.

### 5.4 Ablation Study

More ablation studies are provided in Appendix D.

**Roadmap.** In Tab. 3, we show the roadmap of how to introduce minimal cost to render the causal sequence modeling GLA into proposed ViG. The “improved patch embedding layer” of Row 3 means that instead of directly applying convolution with large  $16 \times 16$  kernel, we adopt a  $9 \times 9$  convolution with stride as 8 followed by  $3 \times 3$  convolution with stride as 2, which only adds 0.03 M parameters but boost the accuracy with nearly no affects on inference efficiency. The ViG-T introduces only 0.11M parameters and significantly outperforms vanilla GLA by 11.1% top-1 accuracy and DeiT by 5.0% top-1 accuracy. By further introducing the hardware-aware bidirectional implementation, we significantly boost the efficiency (enhance throughput by 21.9% and save 13.3% GPU memory) and close the gap with DeiT, even at the low-resolution  $224 \times 224$  image.

**Efficiency of ViG.** In Fig. 4, we compare ViG-T with Vim-T, VRWKV-T, and DeiT-T, focusing on theoretical FLOPs, actual latency, and memory usage on an RTX 4090 GPU. We test the complete

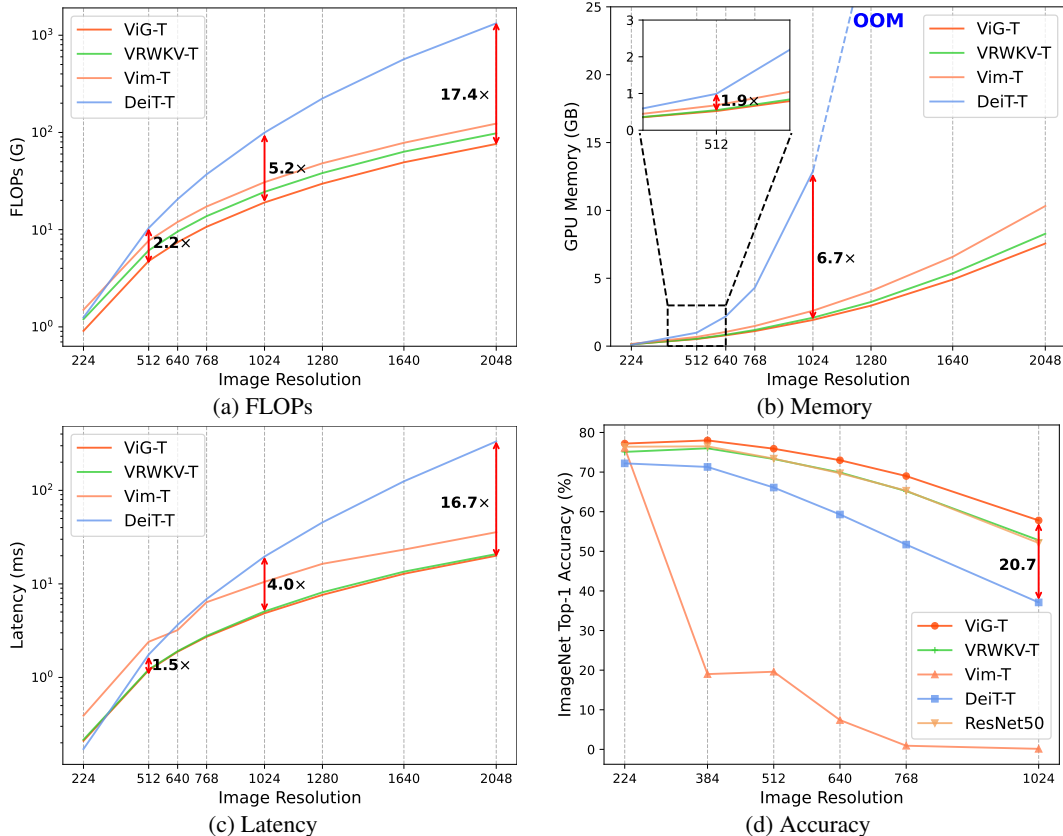


Figure 4: Comparison among ViG, Vim [117], VRWKV [19], and ViT [18, 88] in (a) FLOPs, (b) memory, (c) latency, and (d) accuracy with respect to increasing image resolution during inference on ImageNet-1K val set. The blue dashed line indicates the estimated values when the GPU memory has run out. We benchmark the latency with the maximum batch size that can make models runnable on the GPU to ensure full GPU utilization and provide available results at high resolutions.

model across increasing input image resolutions from  $224 \times 224$  to  $2048 \times 2048$ . Thanks to the linear-complexity sequence modeling, the advantage of the proposed architecture over ViT grows as the resolution increases. When resolution reaches  $1024 \times 1024$ , ViG-T uses  $5.2\times$  lower FLOPs, saves 90% GPU memory, and runs  $4.8\times$  faster than DeiT-T. Compared to its linear-complexity counterpart Vim, ViG also demonstrates  $1.6\times$  lower FLOPs, saves 26% GPU memory, and runs  $2.2\times$  faster. Additionally, ViG surpasses VRWKV in terms of FLOPs, latency, and memory.

**Accuracy vs. Resolution.** In Fig. 4 (d), we test the models trained on  $224 \times 224$  resolution across different resolutions. ViG outperforms ViT, Vim, VRWKV, and even hierarchical CNN-based ResNet50 in terms of accuracy as the resolution increases. The results demonstrate that ViG benefits from better 2D-awareness and demonstrates superior generalization in resolution extrapolation.

## 6 Conclusion

In this paper, we introduced ViG, a generic vision backbone network that introduces Gated Linear Attention (GLA) to the vision field, achieving efficient visual representation learning. Our approach addresses the inherent limitations of traditional Transformers and CNNs by maintaining a global receptive field while operating with linear complexity. We propose direction-wise gating through bidirectional GLA modeling and 2D gating locality injection to effectively capture both global context and local details, leading to significant improvements in accuracy. Additionally, our hardware-aware implementation reduces the overhead brought by extra direction, enhancing efficiency. The superior experimental results of ViG in low-resolution image classification, medium-resolution segmentation, and high-resolution detection highlight it as a very competitive alternative to the existing generic vision backbones.

**Limitations.** Though ViG proposes hardware-aware implementation improves the efficiency, as shown in Tab. 3, and demonstrates obvious superiority at high-resolution input images, it is still slightly inferior to DeiT at the small  $224 \times 224$  input images. We will further optimize the implementation to improve the hardware-awareness in future work.

## Acknowledgement

We would like to acknowledge Yuxin Fang for helpful feedback on the draft.

## References

- [1] Simran Arora, Sabri Eyuboglu, Michael Zhang, Aman Timalsina, Silas Alberti, Dylan Zinsley, James Zou, Atri Rudra, and Christopher Ré. Simple linear attention language models balance the recall-throughput tradeoff. *arXiv preprint arXiv:2402.18668*, 2024.
- [2] Jinze Bai, Shuai Bai, Yunfei Chu, Zeyu Cui, Kai Dang, Xiaodong Deng, Yang Fan, Wenbin Ge, Yu Han, Fei Huang, et al. Qwen technical report. *arXiv preprint arXiv:2309.16609*, 2023.
- [3] Tom Brown, Benjamin Mann, Nick Ryder, Melanie Subbiah, Jared D Kaplan, Prafulla Dhariwal, Arvind Neelakantan, Pranav Shyam, Girish Sastry, Amanda Askell, et al. Language models are few-shot learners. In *NeurIPS*, 2020.
- [4] Guo Chen, Yifei Huang, Jilan Xu, Baoqi Pei, Zhe Chen, Zhiqi Li, Jiahao Wang, Kunchang Li, Tong Lu, and Limin Wang. Video mamba suite: State space model as a versatile alternative for video understanding. *arXiv preprint arXiv:2403.09626*, 2024.
- [5] Hongruixuan Chen, Jian Song, Chengxi Han, Junshi Xia, and Naoto Yokoya. Changemamba: Remote sensing change detection with spatio-temporal state space model. *arXiv preprint arXiv:2404.03425*, 2024.
- [6] Zhe Chen, Yuchen Duan, Wenhai Wang, Junjun He, Tong Lu, Jifeng Dai, and Yu Qiao. Vision transformer adapter for dense predictions. In *ICLR*, 2023.
- [7] Krzysztof Choromanski, Valerii Likhoshesterov, David Dohan, Xingyou Song, Andreea Gane, Tamas Sarlos, Peter Hawkins, Jared Davis, Afroz Mohiuddin, Lukasz Kaiser, et al. Rethinking attention with performers. *arXiv preprint arXiv:2009.14794*, 2020.
- [8] Xiangxiang Chu, Zhi Tian, Yuqing Wang, Bo Zhang, Haibing Ren, Xiaolin Wei, Huaxia Xia, and Chunhua Shen. Twins: Revisiting the design of spatial attention in vision transformers. In *NeurIPS*, 2021.
- [9] Zihang Dai, Hanxiao Liu, Quoc V Le, and Mingxing Tan. Coatnet: Marrying convolution and attention for all data sizes. In *NeurIPS*, 2021.
- [10] Zihang Dai, Zhilin Yang, Yiming Yang, Jaime Carbonell, Quoc V Le, and Ruslan Salakhutdinov. Transformer-xl: Attentive language models beyond a fixed-length context. *arXiv preprint arXiv:1901.02860*, 2019.
- [11] Tri Dao. Flashattention-2: Faster attention with better parallelism and work partitioning. *arXiv preprint arXiv:2307.08691*, 2023.
- [12] Tri Dao, Dan Fu, Stefano Ermon, Atri Rudra, and Christopher Ré. Flashattention: Fast and memory-efficient exact attention with io-awareness. In *NeurIPS*, 2022.
- [13] Soham De, Samuel L Smith, Anushan Fernando, Aleksandar Botev, George Cristian-Muraru, Albert Gu, Ruba Haroun, Leonard Berrada, Yutian Chen, Srivatsan Srinivasan, et al. Griffin: Mixing gated linear recurrences with local attention for efficient language models. *arXiv preprint arXiv:2402.19427*, 2024.
- [14] Jia Deng, Wei Dong, Richard Socher, Li-Jia Li, Kai Li, and Li Fei-Fei. Imagenet: A large-scale hierarchical image database. In *CVPR*, 2009.
- [15] Xiaohan Ding, Xiangyu Zhang, Jungong Han, and Guiguang Ding. Scaling up your kernels to 31x31: Revisiting large kernel design in cnns. In *CVPR*, 2022.
- [16] Xiaohan Ding, Yiyuan Zhang, Yixiao Ge, Sijie Zhao, Lin Song, Xiangyu Yue, and Ying Shan. Unireplenet: A universal perception large-kernel convnet for audio, video, point cloud, time-series and image recognition. In *CVPR*, 2024.

- [17] Xiaoyi Dong, Jianmin Bao, Dongdong Chen, Weiming Zhang, Nenghai Yu, Lu Yuan, Dong Chen, and Baining Guo. Cswin transformer: A general vision transformer backbone with cross-shaped windows. In *CVPR*, 2022.
- [18] Alexey Dosovitskiy, Lucas Beyer, Alexander Kolesnikov, Dirk Weissenborn, Xiaohua Zhai, Thomas Unterthiner, Mostafa Dehghani, Matthias Minderer, Georg Heigold, Sylvain Gelly, et al. An image is worth 16x16 words: Transformers for image recognition at scale. In *ICLR*, 2020.
- [19] Yuchen Duan, Weiyun Wang, Zhe Chen, Xizhou Zhu, Lewei Lu, Tong Lu, Yu Qiao, Hongsheng Li, Jifeng Dai, and Wenhai Wang. Vision-rwkv: Efficient and scalable visual perception with rwkv-like architectures. *arXiv preprint arXiv:2403.02308*, 2024.
- [20] Stéphane d’Ascoli, Hugo Touvron, Matthew L Leavitt, Ari S Morcos, Giulio Biroli, and Levent Sagun. Convit: Improving vision transformers with soft convolutional inductive biases. In *ICML*, 2021.
- [21] Jiemin Fang, Lingxi Xie, Xinggang Wang, Xiaopeng Zhang, Wenyu Liu, and Qi Tian. Msg-transformer: Exchanging local spatial information by manipulating messenger tokens. In *CVPR*, 2022.
- [22] Yuxin Fang, Bencheng Liao, Xinggang Wang, Jiemin Fang, Jiyang Qi, Rui Wu, Jianwei Niu, and Wenyu Liu. You only look at one sequence: Rethinking transformer in vision through object detection. In *NeurIPS*, 2021.
- [23] Yuxin Fang, Quan Sun, Xinggang Wang, Tiejun Huang, Xinlong Wang, and Yue Cao. Eva-02: A visual representation for neon genesis. *arXiv preprint arXiv:2303.11331*, 2023.
- [24] Yuxin Fang, Wen Wang, Binhui Xie, Quan Sun, Ledell Wu, Xinggang Wang, Tiejun Huang, Xinlong Wang, and Yue Cao. Eva: Exploring the limits of masked visual representation learning at scale. In *CVPR*, 2023.
- [25] Yuxin Fang, Shusheng Yang, Shijie Wang, Yixiao Ge, Ying Shan, and Xinggang Wang. Unleashing vanilla vision transformer with masked image modeling for object detection. In *ICCV*, 2023.
- [26] Zhengcong Fei, Mingyuan Fan, Changqian Yu, and Junshi Huang. Scalable diffusion models with state space backbone. *arXiv preprint arXiv:2402.05608*, 2024.
- [27] Daniel Y Fu, Tri Dao, Khaled Kamal Saab, Armin W Thomas, Atri Rudra, and Christopher Re. Hungry hungry hippos: Towards language modeling with state space models. In *ICLR*, 2023.
- [28] Albert Gu and Tri Dao. Mamba: Linear-time sequence modeling with selective state spaces. *arXiv preprint arXiv:2312.00752*, 2023.
- [29] Albert Gu, Karan Goel, and Christopher Ré. Efficiently modeling long sequences with structured state spaces. In *ICLR*, 2022.
- [30] Jianyuan Guo, Kai Han, Han Wu, Yehui Tang, Xinghao Chen, Yunhe Wang, and Chang Xu. Cmt: Convolutional neural networks meet vision transformers. In *CVPR*, 2022.
- [31] Kaiming He, Georgia Gkioxari, Piotr Dollár, and Ross Girshick. Mask r-cnn. In *ICCV*, 2017.
- [32] Kaiming He, Xiangyu Zhang, Shaoqing Ren, and Jian Sun. Deep residual learning for image recognition. In *CVPR*, 2016.
- [33] Xuanhua He, Ke Cao, Keyu Yan, Rui Li, Chengjun Xie, Jie Zhang, and Man Zhou. Pan-mamba: Effective pan-sharpening with state space model. *arXiv preprint arXiv:2402.12192*, 2024.
- [34] Jonathan Ho, Nal Kalchbrenner, Dirk Weissenborn, and Tim Salimans. Axial attention in multidimensional transformers. *arXiv preprint arXiv:1912.12180*, 2019.
- [35] Sepp Hochreiter and Jürgen Schmidhuber. Long short-term memory. *Neural computation*, 1997.
- [36] Qibin Hou, Cheng-Ze Lu, Ming-Ming Cheng, and Jiashi Feng. Conv2former: A simple transformer-style convnet for visual recognition. *arXiv preprint arXiv:2211.11943*, 2022.
- [37] Andrew G Howard, Menglong Zhu, Bo Chen, Dmitry Kalenichenko, Weijun Wang, Tobias Weyand, Marco Andreetto, and Hartwig Adam. Mobilenets: Efficient convolutional neural networks for mobile vision applications. *arXiv preprint arXiv:1704.04861*, 2017.
- [38] Vincent Tao Hu, Stefan Andreas Baumann, Ming Gui, Olga Grebenkova, Pingchuan Ma, Johannes Fischer, and Bjorn Ommer. Zigma: Zigzag mamba diffusion model. *arXiv preprint arXiv:2403.13802*, 2024.

- [39] Gao Huang, Zhuang Liu, Laurens Van Der Maaten, and Kilian Q Weinberger. Densely connected convolutional networks. In *CVPR*, 2017.
- [40] Tao Huang, Xiaohuan Pei, Shan You, Fei Wang, Chen Qian, and Chang Xu. Localmamba: Visual state space model with windowed selective scan. *arXiv preprint arXiv:2403.09338*, 2024.
- [41] Zilong Huang, Xinggang Wang, Lichao Huang, Chang Huang, Yunchao Wei, and Wenyu Liu. Ccnet: Criss-cross attention for semantic segmentation. In *ICCV*, 2019.
- [42] Angelos Katharopoulos, Apoorv Vyas, Nikolaos Pappas, and François Fleuret. Transformers are rnns: Fast autoregressive transformers with linear attention. In *ICML*, 2020.
- [43] Diederik P Kingma and Jimmy Ba. Adam: A method for stochastic optimization. *arXiv preprint arXiv:1412.6980*, 2014.
- [44] Alex Krizhevsky, Ilya Sutskever, and Geoffrey E Hinton. Imagenet classification with deep convolutional neural networks. In *NeurIPS*, 2012.
- [45] Yann LeCun, Léon Bottou, Yoshua Bengio, and Patrick Haffner. Gradient-based learning applied to document recognition. *Proceedings of the IEEE*, 1998.
- [46] Junnan Li, Dongxu Li, Caiming Xiong, and Steven Hoi. Blip: Bootstrapping language-image pre-training for unified vision-language understanding and generation. In *ICML*, 2022.
- [47] Kunchang Li, Xinhao Li, Yi Wang, Yinan He, Yali Wang, Limin Wang, and Yu Qiao. Videomamba: State space model for efficient video understanding. *arXiv preprint arXiv:2403.06977*, 2024.
- [48] Kunchang Li, Yali Wang, Junhao Zhang, Peng Gao, Guanglu Song, Yu Liu, Hongsheng Li, and Yu Qiao. Uniformer: Unifying convolution and self-attention for visual recognition. *TPAMI*, 2023.
- [49] Shufan Li, Harkanwar Singh, and Aditya Grover. Mamba-nd: Selective state space modeling for multi-dimensional data. *arXiv preprint arXiv:2402.05892*, 2024.
- [50] Yanghao Li, Hanzi Mao, Ross Girshick, and Kaiming He. Exploring plain vision transformer backbones for object detection. In *ECCV*, 2022.
- [51] Dingkang Liang, Xin Zhou, Xinyu Wang, Xingkui Zhu, Wei Xu, Zhikang Zou, Xiaoqing Ye, and Xiang Bai. Pointmamba: A simple state space model for point cloud analysis. *arXiv preprint arXiv:2402.10739*, 2024.
- [52] Tsung-Yi Lin, Michael Maire, Serge Belongie, James Hays, Pietro Perona, Deva Ramanan, Piotr Dollár, and C Lawrence Zitnick. Microsoft coco: Common objects in context. In *ECCV*, 2014.
- [53] Hanxiao Liu, Zihang Dai, David So, and Quoc V Le. Pay attention to mlps. In *NeurIPS*, 2021.
- [54] Haotian Liu, Chunyuan Li, Qingyang Wu, and Yong Jae Lee. Visual instruction tuning. In *NeurIPS*, 2024.
- [55] Shiwei Liu, Tianlong Chen, Xiaohan Chen, Xuxi Chen, Qiao Xiao, Boqian Wu, Tommi Kärkkäinen, Mykola Pechenizkiy, Decebal Mocanu, and Zhangyang Wang. More convnets in the 2020s: Scaling up kernels beyond 51x51 using sparsity. In *ICLR*, 2023.
- [56] Yue Liu, Yunjie Tian, Yuzhong Zhao, Hongtian Yu, Lingxi Xie, Yaowei Wang, Qixiang Ye, and Yunfan Liu. Vmamba: Visual state space model. *arXiv preprint arXiv:2401.10166*, 2024.
- [57] Ze Liu, Han Hu, Yutong Lin, Zhuliang Yao, Zhenda Xie, Yixuan Wei, Jia Ning, Yue Cao, Zheng Zhang, Li Dong, et al. Swin transformer v2: Scaling up capacity and resolution. In *CVPR*, 2022.
- [58] Ze Liu, Yutong Lin, Yue Cao, Han Hu, Yixuan Wei, Zheng Zhang, Stephen Lin, and Baining Guo. Swin transformer: Hierarchical vision transformer using shifted windows. In *ICCV*, 2021.
- [59] Zhuang Liu, Hanzi Mao, Chao-Yuan Wu, Christoph Feichtenhofer, Trevor Darrell, and Saining Xie. A convnet for the 2020s. In *CVPR*, 2022.
- [60] Jun Ma, Feifei Li, and Bo Wang. U-mamba: Enhancing long-range dependency for biomedical image segmentation. *arXiv preprint arXiv:2401.04722*, 2024.
- [61] Ningning Ma, Xiangyu Zhang, Hai-Tao Zheng, and Jian Sun. Shufflenet v2: Practical guidelines for efficient cnn architecture design. In *ECCV*, 2018.

- [62] Xuezhe Ma, Xiaomeng Yang, Wenhan Xiong, Beidi Chen, Lili Yu, Hao Zhang, Jonathan May, Luke Zettlemoyer, Omer Levy, and Chunting Zhou. Megalodon: Efficient llm pretraining and inference with unlimited context length. *arXiv preprint arXiv:2404.08801*, 2024.
- [63] Huanru Henry Mao. Fine-tuning pre-trained transformers into decaying fast weights. *arXiv preprint arXiv:2210.04243*, 2022.
- [64] Harsh Mehta, Ankit Gupta, Ashok Cutkosky, and Behnam Neyshabur. Long range language modeling via gated state spaces. In *ICLR*, 2023.
- [65] Tsendsuren Munkhdalai, Manaal Faruqui, and Siddharth Gopal. Leave no context behind: Efficient infinite context transformers with infini-attention. *arXiv preprint arXiv:2404.07143*, 2024.
- [66] Eric Nguyen, Karan Goel, Albert Gu, Gordon W Downs, Preey Shah, Tri Dao, Stephen A Baccus, and Christopher Ré. S4nd: Modeling images and videos as multidimensional signals using state spaces. *arXiv preprint arXiv:2210.06583*, 2022.
- [67] Adam Paszke, Sam Gross, Francisco Massa, Adam Lerer, James Bradbury, Gregory Chanan, Trevor Killeen, Zeming Lin, Natalia Gimelshein, Luca Antiga, et al. Pytorch: An imperative style, high-performance deep learning library. In *NeurIPS*, 2019.
- [68] Badri N Patro and Vijay S Agneeswaran. Simba: Simplified mamba-based architecture for vision and multivariate time series. *arXiv preprint arXiv:2403.15360*, 2024.
- [69] William Peebles and Saining Xie. Scalable diffusion models with transformers. In *ICCV*, 2023.
- [70] Xiaohuan Pei, Tao Huang, and Chang Xu. Efficientmamba: Atrous selective scan for light weight visual mamba. *arXiv preprint arXiv:2403.09977*, 2024.
- [71] Bo Peng, Eric Alcaide, Quentin Anthony, Alon Albalak, Samuel Arcadinho, Huanqi Cao, Xin Cheng, Michael Chung, Matteo Grella, Kranthi Kiran GV, et al. Rwkv: Reinventing rnns for the transformer era. *arXiv preprint arXiv:2305.13048*, 2023.
- [72] Zhen Qin, Xiaodong Han, Weixuan Sun, Dongxu Li, Lingpeng Kong, Nick Barnes, and Yiran Zhong. The devil in linear transformer. *arXiv preprint arXiv:2210.10340*, 2022.
- [73] Zhen Qin, Songlin Yang, Weixuan Sun, Xuyang Shen, Dong Li, Weigao Sun, and Yiran Zhong. Hgrn2: Gated linear rnns with state expansion. *arXiv preprint arXiv:2404.07904*, 2024.
- [74] Zhen Qin, Songlin Yang, and Yiran Zhong. Hierarchically gated recurrent neural network for sequence modeling. In *NeurIPS*, 2024.
- [75] Alec Radford, Jong Wook Kim, Chris Hallacy, Aditya Ramesh, Gabriel Goh, Sandhini Agarwal, Girish Sastry, Amanda Askell, Pamela Mishkin, Jack Clark, et al. Learning transferable visual models from natural language supervision. In *ICML*, 2021.
- [76] Alec Radford, Jeffrey Wu, Rewon Child, David Luan, Dario Amodei, Ilya Sutskever, et al. Language models are unsupervised multitask learners. *OpenAI blog*, 2019.
- [77] Ilija Radosavovic, Raj Prateek Kosaraju, Ross Girshick, Kaiming He, and Piotr Dollár. Designing network design spaces. In *CVPR*, 2020.
- [78] Yongming Rao, Wenliang Zhao, Yansong Tang, Jie Zhou, Ser Nam Lim, and Jiwen Lu. Hornet: Efficient high-order spatial interactions with recursive gated convolutions. In *NeurIPS*, 2022.
- [79] Joseph Redmon and Ali Farhadi. Yolov3: An incremental improvement. *arXiv preprint arXiv:1804.02767*, 2018.
- [80] Mike Schuster and Kuldeep K Paliwal. Bidirectional recurrent neural networks. *TIP*, 1997.
- [81] Noam Shazeer. Glu variants improve transformer. *arXiv preprint arXiv:2002.05202*, 2020.
- [82] Qiuhong Shen, Xuanyu Yi, Zike Wu, Pan Zhou, Hanwang Zhang, Shuicheng Yan, and Xinchao Wang. Gamba: Marry gaussian splatting with mamba for single view 3d reconstruction. *arXiv preprint arXiv:2403.18795*, 2024.
- [83] Jimmy T.H. Smith, Andrew Warrington, and Scott Linderman. Simplified state space layers for sequence modeling. In *ICLR*, 2023.

- [84] Quan Sun, Yuxin Fang, Ledell Wu, Xinlong Wang, and Yue Cao. Eva-clip: Improved training techniques for clip at scale. *arXiv preprint arXiv:2303.15389*, 2023.
- [85] Yutao Sun, Li Dong, Shaohan Huang, Shuming Ma, Yuqing Xia, Jilong Xue, Jianyong Wang, and Furu Wei. Retentive network: A successor to transformer for large language models. *arXiv preprint arXiv:2307.08621*, 2023.
- [86] Mingxing Tan and Quoc Le. Efficientnet: Rethinking model scaling for convolutional neural networks. In *ICML*, 2019.
- [87] Mingxing Tan and Quoc Le. Efficientnetv2: Smaller models and faster training. In *ICML*, 2021.
- [88] Hugo Touvron, Matthieu Cord, Matthijs Douze, Francisco Massa, Alexandre Sablayrolles, and Hervé Jégou. Training data-efficient image transformers & distillation through attention. In *ICML*, 2021.
- [89] Hugo Touvron, Thibaut Lavril, Gautier Izacard, Xavier Martinet, Marie-Anne Lachaux, Timothée Lacroix, Baptiste Rozière, Naman Goyal, Eric Hambro, Faisal Azhar, et al. Llama: Open and efficient foundation language models. *arXiv preprint arXiv:2302.13971*, 2023.
- [90] Zhengzhong Tu, Hossein Talebi, Han Zhang, Feng Yang, Peyman Milanfar, Alan Bovik, and Yinxiao Li. Maxvit: Multi-axis vision transformer. In *ECCV*, 2022.
- [91] Ashish Vaswani, Noam Shazeer, Niki Parmar, Jakob Uszkoreit, Llion Jones, Aidan N Gomez, Łukasz Kaiser, and Illia Polosukhin. Attention is all you need. In *NeurIPS*, 2017.
- [92] Jingdong Wang, Ke Sun, Tianheng Cheng, Borui Jiang, Chaorui Deng, Yang Zhao, Dong Liu, Yadong Mu, Mingkui Tan, Xinggang Wang, et al. Deep high-resolution representation learning for visual recognition. *TPAMI*, 2020.
- [93] Junxiong Wang, Jing Nathan Yan, Albert Gu, and Alexander M Rush. Pretraining without attention. *arXiv preprint arXiv:2212.10544*, 2022.
- [94] Wenhai Wang, Jifeng Dai, Zhe Chen, Zhenhang Huang, Zhiqi Li, Xizhou Zhu, Xiaowei Hu, Tong Lu, Lewei Lu, Hongsheng Li, et al. Internimage: Exploring large-scale vision foundation models with deformable convolutions. In *CVPR*, 2023.
- [95] Wenhai Wang, Enze Xie, Xiang Li, Deng-Ping Fan, Kaitao Song, Ding Liang, Tong Lu, Ping Luo, and Ling Shao. Pyramid vision transformer: A versatile backbone for dense prediction without convolutions. In *ICCV*, 2021.
- [96] Wenhai Wang, Enze Xie, Xiang Li, Deng-Ping Fan, Kaitao Song, Ding Liang, Tong Lu, Ping Luo, and Ling Shao. Pvt v2: Improved baselines with pyramid vision transformer. *Computational Visual Media*, 2022.
- [97] Haiping Wu, Bin Xiao, Noel Codella, Mengchen Liu, Xiyang Dai, Lu Yuan, and Lei Zhang. Cvt: Introducing convolutions to vision transformers. In *ICCV*, 2021.
- [98] Tete Xiao, Yingcheng Liu, Bolei Zhou, Yuning Jiang, and Jian Sun. Unified perceptual parsing for scene understanding. In *ECCV*, 2018.
- [99] Enze Xie, Wenhai Wang, Zhiding Yu, Anima Anandkumar, Jose M Alvarez, and Ping Luo. Segformer: Simple and efficient design for semantic segmentation with transformers. In *NeurIPS*, 2021.
- [100] Saining Xie, Ross Girshick, Piotr Dollár, Zhuowen Tu, and Kaiming He. Aggregated residual transformations for deep neural networks. In *CVPR*, 2017.
- [101] Saining Xie, Ross Girshick, Piotr Dollár, Zhuowen Tu, and Kaiming He. Aggregated residual transformations for deep neural networks. In *CVPR*, 2017.
- [102] Zhaohu Xing, Tian Ye, Yijun Yang, Guang Liu, and Lei Zhu. Segmamba: Long-range sequential modeling mamba for 3d medical image segmentation. *arXiv preprint arXiv:2401.13560*, 2024.
- [103] Jing Nathan Yan, Jiatao Gu, and Alexander M Rush. Diffusion models without attention. *arXiv preprint arXiv:2311.18257*, 2023.
- [104] Chenhongyi Yang, Zehui Chen, Miguel Espinosa, Linus Ericsson, Zhenyu Wang, Jiaming Liu, and Elliot J Crowley. Plainmamba: Improving non-hierarchical mamba in visual recognition. *arXiv preprint arXiv:2403.17695*, 2024.

- [105] Jianwei Yang, Chunyuan Li, Pengchuan Zhang, Xiyang Dai, Bin Xiao, Lu Yuan, and Jianfeng Gao. Focal self-attention for local-global interactions in vision transformers. *arXiv preprint arXiv:2107.00641*, 2021.
- [106] Songlin Yang, Bailin Wang, Yikang Shen, Rameswar Panda, and Yoon Kim. Gated linear attention transformers with hardware-efficient training. In *ICML*, 2024.
- [107] Songlin Yang and Yu Zhang. FLA: A Triton-based library for hardware-efficient implementations of linear attention mechanism. <https://github.com/sustcsonglin/flash-linear-attention>, 2024.
- [108] Yijun Yang, Zhaohu Xing, and Lei Zhu. Vivim: a video vision mamba for medical video object segmentation. *arXiv preprint arXiv:2401.14168*, 2024.
- [109] Weihao Yu, Mi Luo, Pan Zhou, Chenyang Si, Yichen Zhou, Xinchao Wang, Jiashi Feng, and Shuicheng Yan. Metaformer is actually what you need for vision. In *CVPR*, 2022.
- [110] Li Yuan, Yunpeng Chen, Tao Wang, Weihao Yu, Yujun Shi, Zi-Hang Jiang, Francis EH Tay, Jiashi Feng, and Shuicheng Yan. Tokens-to-token vit: Training vision transformers from scratch on imagenet. In *ICCV*, 2021.
- [111] Biao Zhang and Rico Sennrich. Root mean square layer normalization. In *NeurIPS*, 2019.
- [112] Wenqiang Zhang, Zilong Huang, Guozhong Luo, Tao Chen, Xinggang Wang, Wenyu Liu, Gang Yu, and Chunhua Shen. Topformer: Token pyramid transformer for mobile semantic segmentation. In *CVPR*, 2022.
- [113] Xiaosong Zhang, Yunjie Tian, Wei Huang, Qixiang Ye, Qi Dai, Lingxi Xie, and Qi Tian. Hivit: Hierarchical vision transformer meets masked image modeling. *arXiv preprint arXiv:2205.14949*, 2022.
- [114] Zeyu Zhang, Akide Liu, Ian Reid, Richard Hartley, Bohan Zhuang, and Hao Tang. Motion mamba: Efficient and long sequence motion generation with hierarchical and bidirectional selective ssm. *arXiv preprint arXiv:2403.07487*, 2024.
- [115] Sijie Zhao, Hao Chen, Xueliang Zhang, Pengfeng Xiao, Lei Bai, and Wanli Ouyang. Rs-mamba for large remote sensing image dense prediction. *arXiv preprint arXiv:2404.02668*, 2024.
- [116] Bolei Zhou, Hang Zhao, Xavier Puig, Tete Xiao, Sanja Fidler, Adela Barriuso, and Antonio Torralba. Semantic understanding of scenes through the ade20k dataset. *IJCV*, 2019.
- [117] Lianghui Zhu, Bencheng Liao, Qian Zhang, Xinlong Wang, Wenyu Liu, and Xinggang Wang. Vision mamba: Efficient visual representation learning with bidirectional state space model. In *ICML*, 2024.

## A Extended Related Work

**Visual Representation Learning through CNN and Transformer.** Visual representation learning remains a cornerstone of computer vision research, substantially propelled by advancements in deep neural networks. Convolutional Neural Network (CNN) [45] has long been the dominant architecture in this field for its efficient processing of spatial data. It serves as the backbone in many advanced vision encoders [32, 100, 59, 86, 77, 39, 92, 101, 44, 79, 15, 16, 55, 36, 94, 78, 37, 61, 87] across various tasks. Vision Transformer (ViT) [18], a seminal work, challenges the dominance of CNNs by introducing the plain, non-hierarchical Transformer architecture [91] to the vision domain, demonstrating that visual representation learning can effectively be conducted in a pure sequence-to-sequence manner. DeiT [88] further refines ViT by enhancing optimization through advanced training techniques and distillation. To mitigate the notorious issue of quadratic complexity in Transformer softmax attention, the SwinTransformer [58] introduces a hierarchical structure and confines attention computation to local windows, effectively reducing complexity to linear. Similarly, Pyramid Vision Transformer (PVT) [95] employs spatial downsampling on key and value feature maps to decrease the computational demands of global attention. Numerous subsequent studies [97, 96, 105, 9, 20, 21, 30, 17, 90, 112, 57, 110, 8, 113, 48] continue to enhance ViT performance, drawing inspiration from the successes of CNNs.

**Linear Complexity Sequence Modeling.** Transformer [91] has been very successful in sequence modeling, serving as a core module in many state-of-the-art Large Language Models (LLMs) [89, 3, 76, 2] in the NLP field. However, it requires retaining all the historical Key-Value cache and attending the current token to all the historical caches, limiting its application for long sequences. To circumvent this issue, RNN-like sequence modelings [35, 74, 42, 7, 1, 73, 10, 13, 65, 62] attract increasing interest for its merits in linear complexity, fixed hidden state, and global context interaction. RWKV [71] and RetNet [85] introduce temporal decay to model the long-range dependency. Recently, building on SSM [29, 83, 27, 64], Mamba [28] introduces a novel selective SSM operation and demonstrates competitive performance against modern optimized Transformer models with linear complexity. To further improve the practical efficiency, Mamba introduces hardware-aware implementation to reduce the I/O and memory costs. Drawing inspiration from linear attention [42, 63, 72] and retention [85], GLA [106] adds a novel data-dependent gating mechanism to enhance the expressiveness and implements it in a hardware-aware manner [12, 11] to significantly boost efficiency.

**Linear Complexity Visual Sequence Modeling.** Inspired by the success of ViT [18] in visual sequence learning and Mamba [28] in achieving linear complexity in language modeling, Vim [117] introduces the advanced Mamba block to vision by replacing the quadratic softmax attention in ViT with the proposed linear complexity bidirectional SSM [80, 93, 103]. This adaptation demonstrates competitive performance with improved efficiency compared to ViT. Concurrently, VMamba [56] adopts a hierarchical macro architecture similar to SwinTransformer [58] and proposes using the Mamba block to scan the 1D visual sequence in criss-cross patterns [41, 34] for 2D visual representation learning. Numerous follow-up works [38, 104, 40, 70, 49] explore the use of Mamba to scan the 1D visual sequence in more complex 2D-aware patterns. For instance, PlainMamba [104] proposes multiple continuous 2D scannings for 1D visual sequence, while LocalMamba [40] opts for scanning within local windows. In contrast, VisionRWKV [19] forgoes the Mamba block, adapting the linear complexity RWKV block from NLP for use in vision.

## B Architecture Details

We provide detailed configuration of our non-hierarchical ViG and hierarchical ViG-H in Tab. 4.

## C Experimental Details

**ImageNet Classification Experimental Details.** ImageNet contains 1.2M training images and 50K validation images from 1000 categories. We train the models on the training set and report the top-1 accuracy on the validation set. All the model are trained from scratch for 300 epochs, with a cosine schedule and EMA, using a total batch size of 1024. We use AdamW optimizer [43] and set betas to (0.9, 0.999), momentum to 0.9, weight decay to 0.05, initial learning rate to  $1 \times 10^{-3}$ . Images are cropped to  $224 \times 224$  for both training and evaluation. We build upon PyTorch [67] and train Tiny and Small models with  $8 \times 4090$  GPUs, and the Base model with  $16 \times 4090$  GPUs.

Table 4: **Detailed configurations of different variants of ViG.** For hierarchical variants, we provide the number of channels and blocks in 4 stages. The FLOPs are calculated with  $224 \times 224$  input image.

Model	#Blocks	#Channels	#Heads	Params	FLOPs
ViG-T	12	192	3	6M	0.9G
ViG-S	12	384	6	23M	3.5G
ViG-B	12	768	12	89M	13.8G
ViG-H-T	[2, 2, 5, 2]	[96, 192, 384, 768]	[3, 6, 12, 24]	29M	4.5G
ViG-H-S	[2, 2, 17, 2]	[96, 192, 384, 768]	[3, 6, 12, 24]	50M	8.8G
ViG-H-B	[2, 2, 17, 2]	[128, 256, 512, 1024]	[4, 8, 16, 32]	89M	15.5G

Table 5: **Comparison of different bidirectional design.**  $\text{GLA}_{\text{vim}}$  denotes that we follow Vim to build bidirectional modeling on GLA by introducing an extra backward GLA layer. The throughput and memory are measured on a single RTX 4090 GPU with batch size 256 and image size 224 following [58].

Method	#Param.	Throughput	Mem.	Top-1 Acc.
GLA	5.72M	6662	582MB	66.1
$\text{GLA}_{\text{vim}}$	6.70M	4524	812MB	73.5
ViG	5.83M	4645	730MB	77.2

**ADE20K Semantic Segmentation Experimental Details.** All the models are initialized with ImageNet-1K pre-trained weights. Training details follow the setting in VRWKV [19]. We employ the AdamW optimizer, setting initial learning rate to  $6 \times 10^{-5}$  for the Small/Base models and  $1.2 \times 10^{-4}$  for the Tiny model, a batch size of 16, and a weight decay of 0.01. We train all the models for 160k iterations on the training set of the ADE20K dataset.

**COCO Object Detection Experimental Details.** All models are initialized with ImageNet-1K pre-trained weights and trained according to a 12-epoch schedule with a batch size of 16. We follow VRWKV [19] and employ the AdamW optimizer with a learning rate of  $1 \times 10^{-4}$  and a weight decay of 0.05.

## D Ablation Study

**Bidirectional Design.** As shown in Tab. 3, the proposed bidirectional design by applying direction-wise gating  $\bar{\alpha}$  introduces only 0.02M parameters but achieves an improvement of 0.9% in top-1 accuracy without compromising efficiency. In Tab. 5, we introduce another variant,  $\text{GLA}_{\text{vim}}$ , which follows the bidirectional design of Vim [117] by incorporating an extra backward GLA layer, adding nearly 1M parameters. The results demonstrate that the proposed bidirectional modeling and implementation is faster, more parameter-efficient, more memory-efficient, and more accurate than Vim.

**Gating Mechanism Understanding.** In Fig. 5, we visualize the attention maps of the proposed BiGLA layer. The results show that the forward and backward attention complement each other, and the merged attention can capture the prominent 2D context of the images.

**Effective Receptive Field Analysis.** In Fig. 6, we compare the effective receptive field (ERF) of different models, including CNN-based ResNet50, window-attention-based SwinTransformer, vanilla ViT variant DeiT. The results show that the ViG exhibits a global ERF like DeiT, while the CNN-based and window-attention-based methods fail. We also visualize the ERF of variant  $\text{BidGLA}_{\bar{\alpha}}$ , which only applies direction-wise gating  $\bar{\alpha}$  (Row 6 in Tab. 3). The results demonstrate that the proposed 2D locality injection enlarges the area of intensive response, which is beneficial for capturing the spatial-aware context.

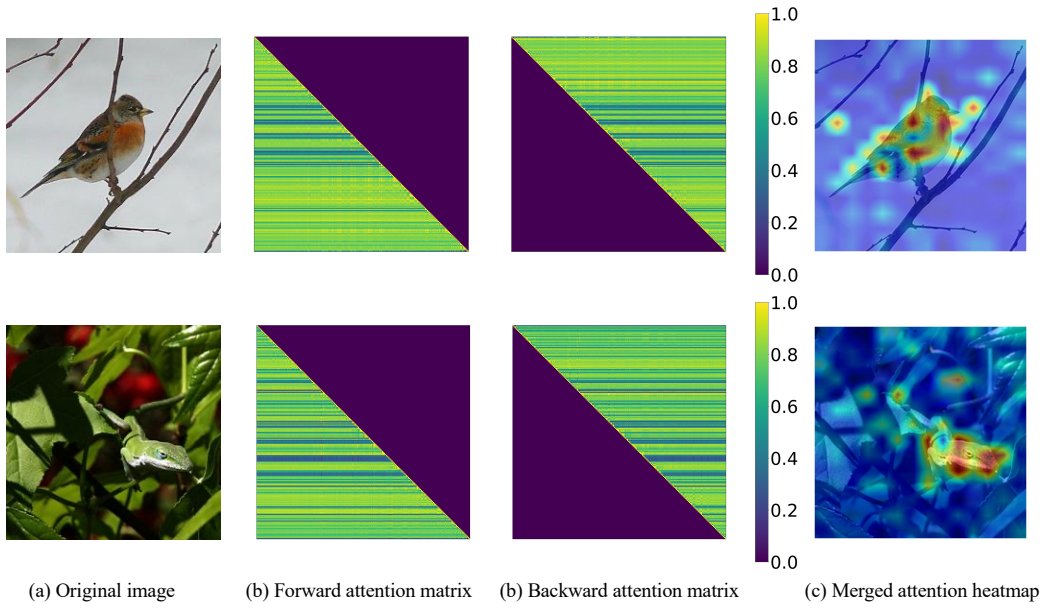


Figure 5: Visualization of attention maps.

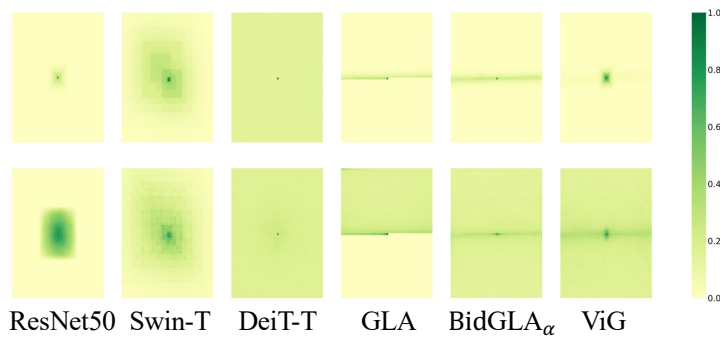


Figure 6: Comparison of Effective Receptive Field (ERF). “BidGLA $_{\bar{\alpha}}$ ” denotes the proposed bidirectional design with direction-wise gating  $\bar{\alpha}$  (Row 4 in Tab. 3). The proposed ViG and BidGLA $_{\bar{\alpha}}$  exhibit a global ERF like DeiT. By introducing the 2D locality injection, the area of intensive response is larger.